PHYSICAL REVIEW A **71**, 061803(R) (2005)

Noise-free high-efficiency photon-number-resolving detectors

Danna Rosenberg, Adriana E. Lita, Aaron J. Miller, and Sae Woo Nam
National Institute of Standards and Technology, 325 Broadway, Boulder, Colorado 80305, USA

(Received 21 March 2005; revised manuscript received 15 April 2005; published 17 June 2005; publisher error corrected 21 June 2005)

High-efficiency optical detectors that can determine the number of photons in a pulse of monochromatic light have applications in a variety of physics studies, including post-selection-based entanglement protocols for linear optics quantum computing and experiments that simultaneously close the detection and communication loopholes of Bell's inequalities. Here we report on our demonstration of fiber-coupled, noise-free, photon-number-resolving transition-edge sensors with 88% efficiency at 1550 nm. The efficiency of these sensors could be made even higher at any wavelength in the visible and near-infrared spectrum without resulting in a higher dark-count rate or degraded photon-number resolution.

DOI: 10.1103/PhysRevA.71.061803 PACS number(s): 42.50.Ar, 85.25.Pb, 85.25.Oj

High-efficiency, photon-number-resolving detectors can transform the field of quantum optics. One of many experiments they can enable is linear optics quantum computing, which requires postselection based on photon number [1]. So far, researchers have succeeded in implementing simple two-qubit gates by using conventional detectors that cannot distinguish between one and two photons [2,3], but moving beyond two qubits requires high-efficiency, low dark-count rate, photon-number-resolving detectors. Such detectors can be used to herald multiphoton path-entangled states from the output of a parametric down-conversion crystal [4], and these entangled states could be used for applications ranging from quantum cryptography [5,6] to lithography beyond the diffraction limit [7].[1] Photon-number-resolving detectors can also be used to verify the quality of single-photon sources, a necessity for secure information transfer in some quantum key distribution protocols. Furthermore, low-noise, high-efficiency detectors that operate at telecommunication wavelengths can significantly extend the length of a secure link in fiber quantum key distribution where light must be transmitted over large distances [8].

Conventional detectors that operate in the visible and near infrared, such as avalanche photodiodes and photomultiplier tubes, may be single-photon sensitive, but they cannot reliably determine the number of photons in a pulse of light [9–11]. In principle, beam splitters and single-photon sensitive detectors can simulate a photon-number-resolving detector [12], but the probability of correctly identifying an N-photon event drops exponentially with N, even for detectors with 100% efficiency, because it is impossible to control the path each photon takes at a beam splitter. Novel technologies such as the visible-light photon counter [13] have some photon-number-resolution ability, but operating them at maximum detection efficiency introduces dark counts at rates greater than 10 kHz, and these detectors are sensitive in the visible spectrum only.

Superconducting transition-edge sensors (TESs) have photon-number resolution with negligibly low dark counts. The TESs discussed in this paper are quantum calorimeters optimized for detection of near-infrared and visible photons [14–16]. The main components of a calorimeter are the absorber, a thermometer, and a weak link to a thermal heat sink, as shown in Fig. 1. When energy impinges on the absorber, it heats up quickly and slowly cools through the weak thermal link, and the temperature change is measured by the thermometer. Detection of visible and near-infrared light at the single-photon level places stringent requirements on the heat capacity and thermometry. For the TESs described here, the electron subsystem in a thin film of tungsten plays the parts of both the absorber and thermometer. The detector is cooled below its superconducting transition temperature and a voltage bias is applied to increase the electron temperature above that of the substrate. At low temperatures, the electrons in tungsten have anomalously low thermal coupling to the phonons, providing the weak thermal link, and the rapid change in resistance near the superconducting critical temperature results in a very sensitive measure of temperature. The temperature change due to energy deposition by a photon results in a change in resistance, and the current change in the voltage-biased detector is measured with a superconducting quantum-inteference device (SQUID) array [17].

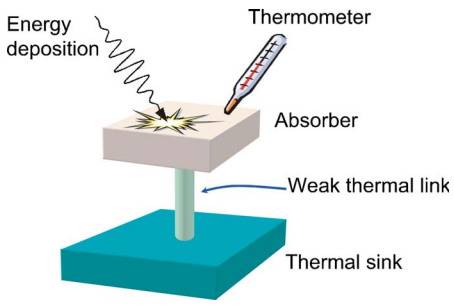

FIG. 1. (Color online) Calorimeter operation. Energy is deposited in the absorber and the thermometer reads out the change in temperature. The absorber cools down slowly through the weak link to the thermal heat sink. The tungsten transition-edge sensors discussed in this paper are quantum calorimeters, with the tungsten electrons acting as both the absorber and thermometer. A voltage bias keeps the tungsten electrons on the edge of the superconducting-to-normal transition, and the steep dependence of resistance on temperature provides precise thermometry. The anomalously low electron-phonon coupling in tungsten is the weak thermal link.

[1] In order to be practical, quantum lithography requires the development of a *bright* source of entangled photons.

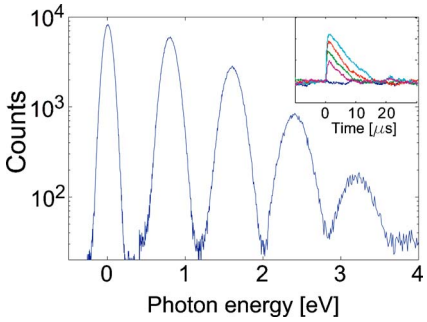

FIG. 2. (Color online) Histogram of corrected pulse heights. The sensor was illuminated with a 1550-nm (0.8-eV) gain-switched laser diode pulsed at 50 kHz with a pulse duration of 4 ns. The pulses from the detector were shaped with a 2-μs semi-Gaussian filter and the maximum value for each pulse was determined. (For events in the zero-photon peak, the amplitude of the signal was measured at the expected arrival time of the photon.) The relationship between filtered pulse height and energy was determined by measuring the mean of each histogram peak, and the data were then corrected to linearize the response of the detector. The full width at half maximum of the zero-, one-, two-, three-, and four-photon peaks are 0.13, 0.20, 0.25, 0.34, and 0.45 eV, respectively. The inset shows typical unfiltered pulses for zero-, one-, two-, three-, and four-photon events.

The change in temperature (and thus current) is proportional to the photon energy, so the sensor can resolve the number of photons in a pulse of monochromatic light.

The detection efficiency of a bare thin-film tungsten sensor 20-nm thick is 15 to 20 % at visible and near-infrared wavelengths and is limited by reflection from the front surface and transmission through the film. However, every photon that is absorbed by the tungsten leads to a change in temperature of the electrons, so the detection probability can be increased by embedding the tungsten detector in a stack of optical elements that enhance the absorption of the light in the tungsten. The TESs discussed in this paper measure 25×25 μm^2 and are approximately 20-nm thick with superconducting critical temperatures of 110 ± 5 mK. They are embedded in structures that are designed to maximize absorption at 1550 nm, a wavelength of particular interest for telecommunications. Existing semiconductor-based detectors have low (10-20 %) efficiency and high (10-20 kHz) dark-count rates at this wavelength. A detailed description of the structures is presented elsewhere [18]. These sensors have thermal decay times as short as 5 μs and provide excellent discrimination between multiphoton events. Figure 2 shows data from a TES embedded in an optical structure designed to enhance the absorption of light at a wavelength of 1550 nm. The sensor was illuminated with a pulsed source of 1550 nm photons. The histogram displays the distribution of pulse heights after the data were corrected for the nonlinearity in the temperature dependence of the resistance in the superconducting transition. The full width at half maximum (FWHM) of the zero-, one-, two-, three-, and four-photon peaks are 0.13, 0.20, 0.25, 0.34, and 0.45 eV, respectively. The increase in the FWHM of the peaks with increasing energy is due to the device nonlinearity mentioned above. Measurements and simulations of the optical properties of the various layers indicate that the total expected efficiency of the sensor, neglecting system losses, is 92%.

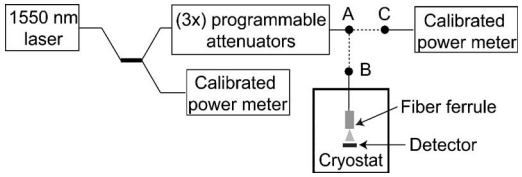

FIG. 3. Experimental apparatus for the detector efficiency measurement. Light from the laser was split into two paths by a fiber coupler. The top path contained three programmable attenuators. A calibrated power meter at point *A* was used to measure the actual attenuation value at every attenuation set point used in the experiment. After the attenuators were calibrated, the fiber exiting the last attenuator was cut at point *A* and fused to the fiber (point *B*) leading to the detector. The power in the bottom arm of the fiber coupler was continuously monitored to ensure that the laser power did not drift. All measurements were performed within the linear range of the power meter.

Photons were coupled to the detector through a 9-μm core single-mode fiber with an antireflective coating for 1550 nm. The fiber was held $50-75$ μm above the detector and aligned at room temperature by backside through-chip imaging. Focusing the light from the fiber was not necessary because the spot size was small enough at this distance, that greater than 99% of the light was incident on the detector. The housing holding the fiber was clamped in place and the detector was then cooled to less than 100 mK in an adiabatic demagnetization refrigerator. Because the applied voltage bias keeps the electrons in the superconducting-to-normal transition, the detector is not sensitive to slight fluctuations in the cryostat temperature as long as the temperature is well below the superconducting transition temperature of 110 ± 5 mK.

Coupling and alignment losses reduce the measured efficiency of the detector from the expected 92%. To minimize connection losses, the fiber from the detector and the fiber going to room temperature were fused together in the cold space of the cryostat. The typical loss for a fiber fuse is approximately 0.5%. We measured the room-temperature loss from outside the cryostat to the sample space to be 2.3%. Tests to determine the loss in a loop of fiber that passes through the cold space of the refrigerator indicated that the loss does not change when the fiber is cooled. Thermal cycling of the fiber-coupled detector did not change its efficiency, and we measured greater than 80% efficiency for several different detectors, indicating that our alignment method is robust and that the fiber-to-detector alignment does not degrade when cooled.

Measuring the efficiency of the detectors is nontrivial due to the low power levels involved and the introduction of loss through fiber connectors. The relatively slow pulse decay (several microseconds) and the desire to avoid pulse pileup requires the use of subfemtowatt average optical power levels. At present, commercial power meters do not have the sensitivity required to measure such low levels. To circumvent this problem, we calibrated a series of programmable optical attenuators using a calibrated power meter well within its linear regime, as shown in Fig. 3. The attenuator

calibration and efficiency measurements were performed using a laser with a center wavelength of 1550 nm and FWHM of 0.05 nm.

The efficiency measurements presented here were performed in continuous-wave operation at several different power levels to ensure that there was no dependence of measured efficiency on power level, as shown in Fig. 4. Power levels were adjusted by means of the calibrated programmable attenuators. The number of pulses with pulse heights within $\pm 3\sigma(\sigma \approx 0.07$ eV) of the one-photon peak was recorded at each power level for 100 s. The background rate in the same energy range, which was approximately 400 Hz and was due to blackbody radiation from room-temperature surfaces [19],[2] was measured periodically between data sets and subtracted from the raw count rate. The procedure outlined above provides a measure of the number of single-photon events from the laser. At the higher power levels, counts were present at energies greater than 3σ above the mean energy of the one-photon peak. The spectral weight at these energies results from pulse pileup, the arrival of a second photon before the system has recovered from a previous event. To correct for this effect, we included the high-energy counts as two-photon events. This correction is smallest (1% of the total counts) at the lowest power levels and remains below 2% at even the highest power level.

Figure 4 shows the detection efficiency as a function of power level, with error bars given by the uncertainties due to Poisson statistics. Not shown are the uncertainties resulting from fiber bends at room temperature. We have observed that small bends in the fiber can easily lower the measured efficiency by up to 3%, and the scatter in efficiency measurements is most likely due to slight shifts in the fiber position. All the efficiency values presented are relative to the amount of light in the fiber at point *A* in Fig. 3.

The measured system efficiency of $88.6 \pm 0.4\%$ is consistent with measurements and simulations of the optical elements and the system losses. This detection efficiency exceeds the threshold of 83% required to close the detection loophole in an experiment testing Bell's inequalities. This enables an experiment that would simultaneously close both the detection and communication loopholes, decisively refuting a local realism interpretation of quantum mechanics.

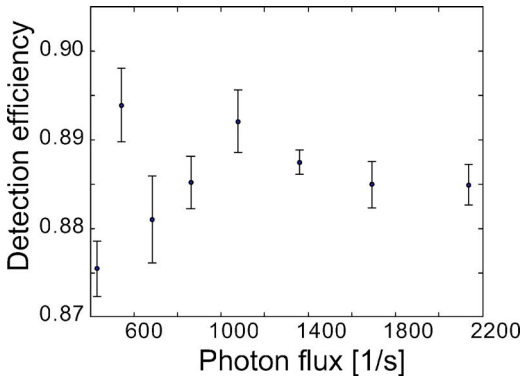

FIG. 4. Detection efficiency. The efficiency was measured at several different average power levels with the laser in continuous-wave operation. The error bars show the statistical counting errors only. The slope of a weighted linear fit to the data is zero within the error bars, indicating that there is no dependence of efficiency on power level. A weighted average of the data yields an efficiency of 88.6% with a combined uncertainty of 0.4%.

Increasing the detection efficiency beyond 88.6% at 1550 nm is in principle simple and involves fabricating an optical structure with more layers and finer control over layer thickness. Similarly, it should be possible to produce near-unity-efficiency detectors at any wavelength in the ultraviolet to near-infrared frequency range with this technique. Simulations indicate the possibility of increasing the efficiency well above 99% at any given wavelength in this spectrum, making these detectors an extremely valuable tool for quantum optics and quantum-information processing.

The authors thank ARDA for financial support; Alan Migdall, Richard Mirin, John Martinis, Alexander Sergienko, and Erich Grossman for valuable technical discussions; and Marty Gould of Zen Machining. D. R. is supported by the DCI postdoctoral program.

[2]Note that the background counts were not from detector noise; rather, they resulted from photons from the low-energy tail of the blackbody distribution propagating through the optical fiber.

[1] E. Knill, R. Laflamme, and G. J. Milburn, Nature (London) **409**, 46 (2001).
[2] S. Gasparoni, J. W. Pan, P. Walther, T. Rudolph, and A. Zeilinger, Phys. Rev. Lett. **93**, 020504 (2004).
[3] J. L. O'Brien, G. J. Pryde, A. G. White, T. C. Ralph, and D. Branning, Nature (London) **426**, 264 (2003).
[4] H. S. Eisenberg, J. F. Hodelin, G. Khoury, and D. Bouwmeester, Phys. Rev. Lett. **94**, 090502 (2005).
[5] A. K. Ekert, Phys. Rev. Lett. **67**, 661 (1991).
[6] C. H. Bennett, G. Brassard, and N. D. Mermin, Phys. Rev. Lett. **68**, 557 (1992).
[7] A. N. Boto, P. Kok, D. S. Abrams, S. L. Braunstein, C. P. Williams, and J. P. Dowling, Phys. Rev. Lett. **85**, 2733 (2000).
[8] N. Lutkenhaus, Acta Phys. Slov. **49**, 549 (1999).
[9] W. G. Oldham, R. R. Samuelson, and P. Antognetti, IEEE Trans. Electron Devices **ED-19**, 1056 (1972).
[10] R. Engstrom, *Photomultiplier Handbook* (RCA, Princeton, NJ, 1980).
[11] B. Levine and C. Bethea, Appl. Phys. Lett. **44**, 553 (1984).
[12] D. Achilles, C. Silberhorn, C. Sliwa, K. Banaszek, I. A. Walmsley, M. J. Fitch, B. C. Jacobs, T. B. Pittman, and J. D. Franson, J. Mod. Opt. **51**, 1499 (2004).
[13] E. Waks, K. Inoue, W. D. Oliver, E. Diamanti, and Y. Yamamoto, IEEE J. Sel. Top. Quantum Electron. **9**, 1502 (2003).
[14] K. D. Irwin, Appl. Phys. Lett. **66**, 1998 (1995).
[15] B. Cabrera, R. M. Clarke, P. Colling, A. J. Miller, S. Nam, and

R. W. Romani, Appl. Phys. Lett. **73**, 735 (1998).
[16] A. J. Miller, S. W. Nam, J. M. Martinis, and A. V. Sergienko, Appl. Phys. Lett. **83**, 791 (2003).
[17] M. E. Huber, P. A. Neil, R. G. Benson, D. A. Burns, A. M. Corey, C. S. Flynn, Y. Kitaygorodskaya, O. Massihzadeh, J. M. Martinis, and G. C. Hilton, IEEE Trans. Appl. Supercond. **11**, 1251 (2001).
[18] D. Rosenberg, A. E. Lita, A. J. Miller, S. Nam, and R. E. Schwall, IEEE Trans. Appl. Supercond. (to be published).
[19] A. J. Miller *et al.* (unpublished).